

Synthesis of flower-like CuO hierarchical nanostructures as an electrochemical platform for glucose sensing

Natália Goedel Medeiros¹ · Vanessa Cezar Ribas¹ · Vladimir Lavayen¹ ·
Jacqueline Arguello Da Silva¹

Received: 6 October 2015 / Revised: 14 February 2016 / Accepted: 17 February 2016 / Published online: 24 February 2016
© Springer-Verlag Berlin Heidelberg 2016

Abstract Flower-like CuO hierarchical nanostructures were synthesized on copper foil substrate through a simple wet chemical route in alkaline media at room temperature. SEM images collected at different reaction times revealed the transformation of initially formed Cu(OH)₂ nanowires to flower-like CuO nanostructures. The hierarchical structure of the as-prepared CuO showed high electrocatalytic activity towards the oxidation of glucose making it a promising electrode material for the development of non-enzymatic glucose sensor. The amperometric sensor exhibited a wide linear response to glucose ranging from 4.5×10^{-5} to 1.3×10^{-3} mol L⁻¹ ($R^2 = 0.99317$) at fixed potential of 0.3 V. The detection limit was 6.9×10^{-6} mol L⁻¹ (LOD = $3\sigma/s$) with a sensitivity of $1.71 \mu\text{A } \mu\text{mol}^{-1} \text{cm}^{-2}$. Moreover, the developed sensor offers a fast amperometric response, good selectivity and stability.

Keywords CuO · Hierarchical nanostructure ·
Electrocatalysis · Glucose sensor

Introduction

Metal oxide nanostructures have attracted considerable attention because of their outstanding properties and numerous technological applications [1–3]. They exhibit size-dependent features, i.e. at the nanometer scale, their properties significantly differ from their bulk material, conferring them new optical, magnetical and electronic characteristics. Among these metal

oxides, copper oxide (CuO) is an important *p*-type semiconductor that exhibits a narrow band gap (1.2–2.6 eV) [4, 5]. Thanks to its unique properties such as high stability and excellent electrical conductivity, CuO finds applications in the fields of catalysis, fuel cells, electronics, batteries and sensors [6–8]. Based on their high surface-to-volume ratio, efficient electron transport properties and low-cost, CuO nanostructures are extensively investigated as electrode material for the development of non-enzymatic glucose sensors [9–12].

The Cu(III)/Cu(II) redox couple mediates the electrocatalytic oxidation of glucose. The effect of the morphologies on the electrochemical performance has stimulated the development of many different approaches to synthesize a great variety of CuO nanostructures. For example, Wang et al. electrodeposited copper nanoparticles/poly(o-phenylenediamine) composite onto glassy carbon electrode [11]. Ibupoto et al. prepared CuO nanosheets on a gold-coated glass substrate by a hydrothermal method [12]. Yang et al. showed the formation of a hollow CuO polyhedron using a Cu₂O-templated growth approach [13]. Kim et al. reported the synthesis of CuO and single-walled carbon nanotubes (SWCNTs) nanocomposite via simultaneous arc discharging of Cu and graphite followed by oxidation [14]. Another simple approach consists in the synthesis of CuO on copper foil substrates via Cu oxidation in an alkaline medium by a simple wet chemical route at room temperature. By following this method, Chattopadhyay et al. obtained CuO with different morphologies, nanoneedles, nanoflowers and staked flake-like structures depending on the pH solution [15]. These are just some examples among the many possibilities for the development of CuO nanostructures.

In spite of their good accuracy and precision, enzymatic biosensors for glucose detection still suffer some limitations resulting from the dependency of enzyme's activity on the temperature, humidity, pH, etc. Thus, in the last decades, considerable attention has been directed towards the development

✉ Jacqueline Arguello Da Silva
jacqueline.arguello@ufrgs.br

¹ Institute of Chemistry, Federal University of Rio Grande do Sul, Porto Alegre, RS, Brazil

of non-enzymatic glucose sensors [16, 17]. This way, metal oxides, hybrid metal oxides, noble metals, graphene, carbon nanotubes, polymers and other composites have been explored for application in glucose sensors.

Although that graphene-, noble metals- and carbon nanotubes-based sensors are highly sensitive, selective, stable and reproducible, they are expensive compared to other materials, especially copper. This metal is low-cost, and as mentioned above, CuO nanostructures can be readily formed on its surface making it a suitable material for glucose electrooxidation.

In this study, flower-like hierarchical nanostructures of CuO were prepared on a copper foil via a template-free wet chemical method in an alkaline medium. The as-synthesized material showed excellent electrocatalytic properties towards the oxidation of glucose, pointing out its potential usefulness as working electrode for the development of glucose sensor.

Experimental

Materials and reagents

All reagents were of analytical grade and used as received without any further purification: hydrochloric acid, absolute

ethanol, ammonium hydroxide solution and sodium hydroxide. Copper foil was purchased from Sigma-Aldrich, with 99.98 % purity and 0.25 mm of thickness. All solutions were prepared using a deionized water of resistivity not less than 18.2 M Ω cm (Milli-Q purification system, Millipore). The electrochemical studies were performed using 0.1 mol L⁻¹ NaOH as the supporting electrolyte. Glucose standard solutions were freshly prepared before each measurement.

Synthesis of flower-like CuO hierarchical nanostructures

The in situ oxidation process allows the formation of flower-like CuO hierarchical nanostructures on copper foil, as previously described [15]. In a typical procedure, the copper foil was firstly pre-treated to remove the impurities from the metal surface, as well as oxide layers. Cu (0.5 cm \times 1.0 cm) was washed with 4 mol L⁻¹ HCl solution for 15 min and then with ultra-pure water and absolute ethanol. The treated copper foil was then immersed in a solution consisting of 0.0125 mol L⁻¹ NaOH and 0.0975 mol L⁻¹ NH₃·H₂O (pH = 11.5). The reaction proceeds for a period ranging from 6 to 96 h at 22 °C. Two replicate experiments were conducted to assess the reproducibility. After the reaction time, the sample was removed, washed with deionized water and dried in air at 60 °C for 3 h. For the electrodes, the 96 h reaction time was chosen

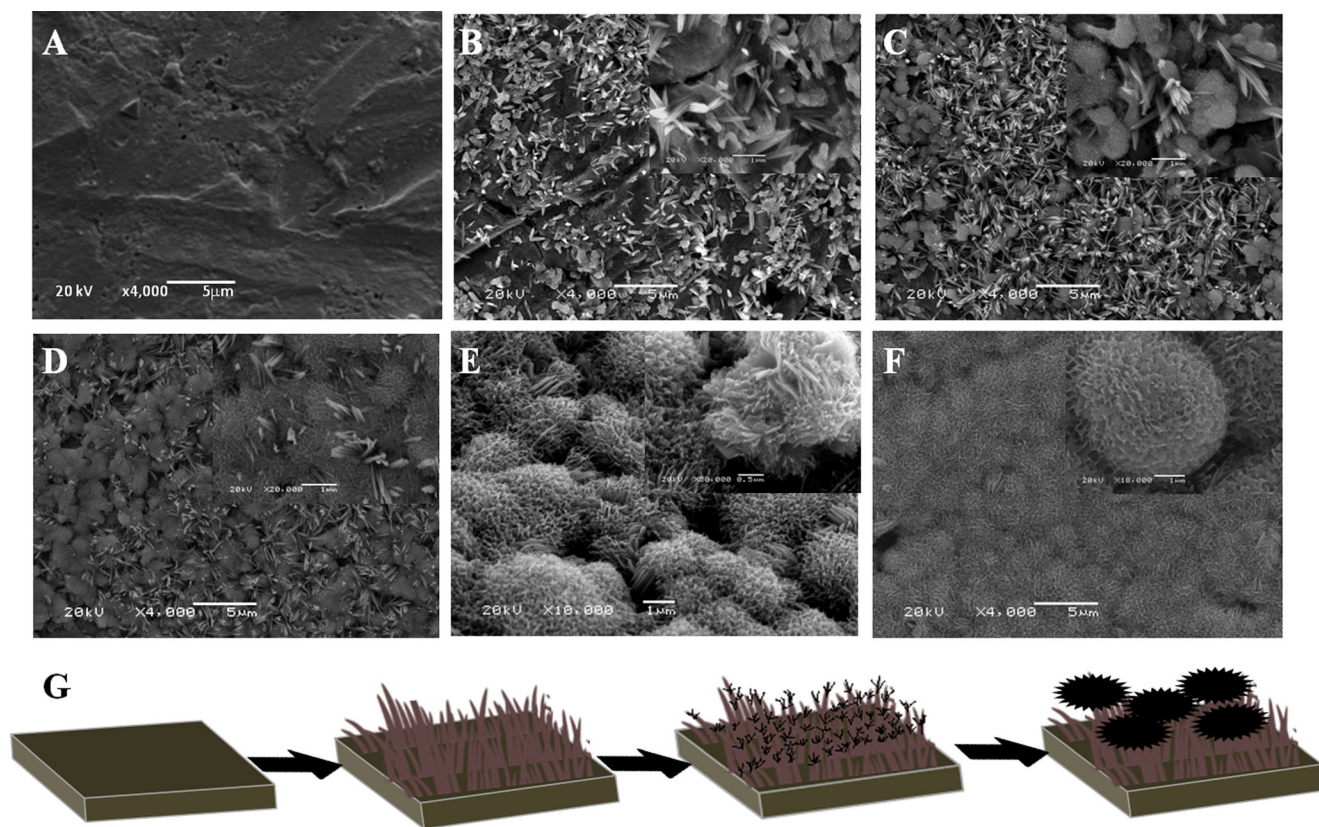


Fig. 1 SEM images of CuO at different reaction times: 0 h (a), 6 h (b), 15 h (c), 24 h (d), 68 h (e), 96 h (f) and schematic representation of the growth process of the flower-like CuO hierarchical nanostructure (g)

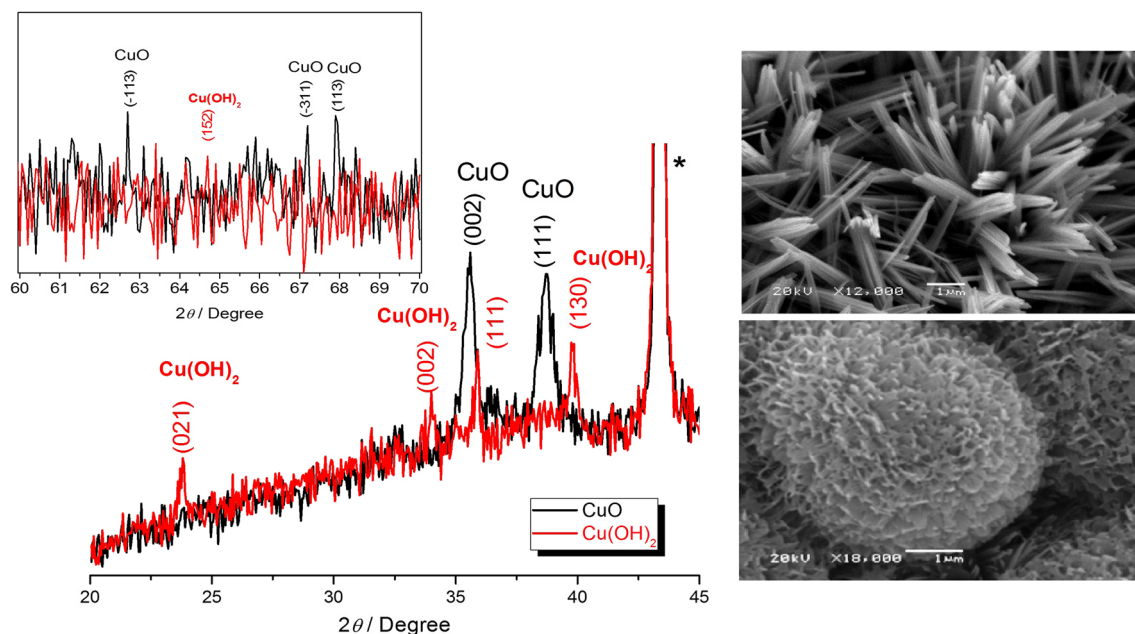


Fig. 2 XRD patterns of the flower-like CuO hierarchical nanostructure and Cu(OH)₂ nanowires with their respective SEM images. Peak mark with asterisk correspond to Cu foil

due to the homogeneous and complete coverage. Also, a larger piece of copper (0.5 cm × 2.0 cm) was used for the electrode to make the electric contact and the experiment was performed in triplicate. The geometric area of the CuO electrode was 0.5 × 0.5 cm.

Characterization

The morphologies of the as-grown CuO were investigated by scanning electron microscopy (SEM) using a JEOL JSM-6060 instrument operated at 20 kV. X-ray diffraction (XRD) pattern was obtained by a Rigaku D-Max 2000 equipment operated at 30 kV voltage and 15 mA current using a monochromatic Cu K_α radiation ($\lambda = 1.5406 \text{ \AA}$) in the range 20–70°. The electrochemical measurements were performed

using a potentiostat (Autolab, PGSTAT302N model). The cell consists of a system of three electrodes, the synthesized working electrode, a platinum wire as the counter electrode and saturated calomel electrode as the reference electrode.

Results and discussion

Characterization of the flower-like CuO structures

SEM images were registered at different reaction times to monitor the evolution in the formation of the flower-like structures on the copper foil. Fig. 1(a–f) reveals the morphology of the copper surface before the immersion in the alkaline solution (a) and after 6, 15, 24, 68 and 96 h of reaction times (b–f).

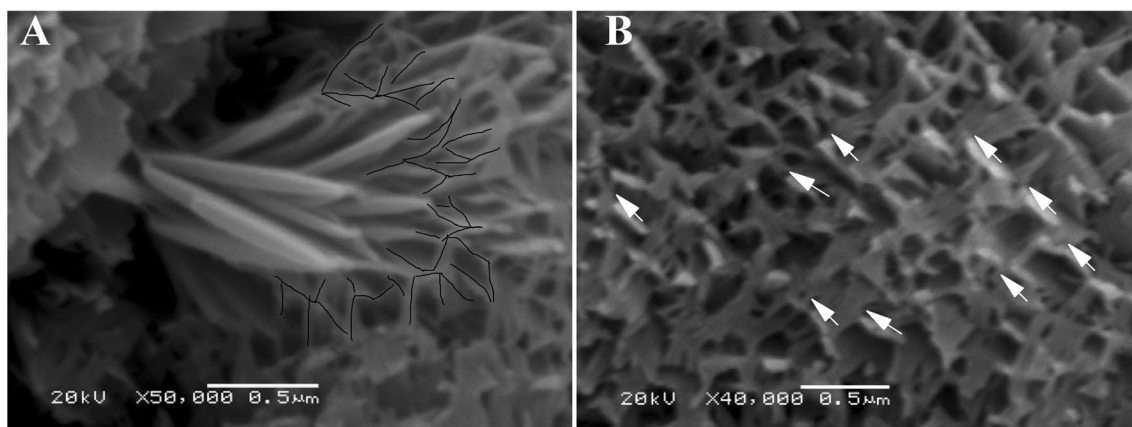


Fig. 3 Enlarged SEM images revealing the flower-like structure of CuO. **a** At the edge of the stacked nanowires can be observed the ramification from which the morphology starts to change. **b** The image of the top view exhibits the orientated growth of CuO in a 3D structure (the arrowheads)

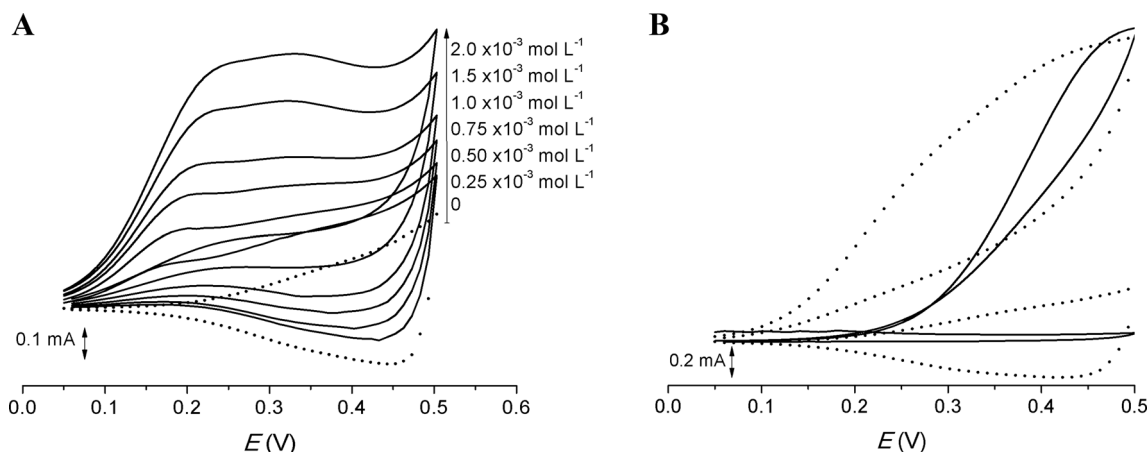
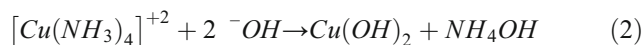
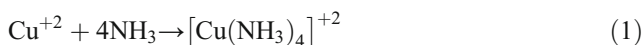


Fig. 4 **a** CVs for the CuO electrode recorded in the absence (*dotted line*) and the presence (*solid line*) of glucose (0.25, 0.50, 0.75, 1.0, 1.5 and 2.0×10^{-3} mol L⁻¹). **b** CVs for the CuO electrode (*dotted line*) and

untreated copper electrode (*solid line*) recorded in the absence and the presence of 5.0×10^{-3} mol L⁻¹. 0.1 mol L⁻¹ NaOH and scan rate of 10 mV s⁻¹

After the 6 h of reaction, the metal is covered but not completely by grass-like nanowires (Fig 1b). As the reaction proceeds, a full coverage is achieved, but at this time concomitantly with the nanowires starting to appear another kind of arrangement (Fig. 1c). It seems that thinner and shorter nanowires start branching out and forming agglomerates. At 24 h of reactions, these structures become predominant (Fig. 1d). Subsequent growth of these agglomerated structures leads to the formation of 3D flower-like architectures (Fig. 1e–f). Based on this time-dependent experiment, a growth mechanism of CuO is proposed in Fig. 1f, drawing the different stages starting from the formation of nanowires until the achievement of the flower-like hierarchical structures. According to the reported references [15, 18], the chemical reactions involved in the growth of CuO by the treatment of copper foils with NH₃·H₂O and NaOH is as follows:



It is known that the oxidation of copper in the air or under humid conditions proceeds very slowly, but the presence of alkali solutions dramatically accelerates the reactions. In the initial stage of the reaction, the copper foil releases Cu⁺² ions into the solution forming the [Cu(NH₃)₄]⁺² complex (Eq. 1). The high ⁻OH concentration causes the formation of Cu(OH)₂ which subsequently dehydrates producing CuO (Eq. 2–3). As a precursor, the presence of Cu(OH)₂ may become apparent at short reaction times. Thus, the observed nanowires can be strongly associated with the layered structure of orthorhombic Cu(OH)₂. According to previous studies, Cu(OH)₂ has a preferred growth direction and usually form one-dimensional nanostructures [19, 20]. Since the reaction also depends on

the temperature, another reaction was performed at 4 °C, attempting this time to obtain the Cu(OH)₂ nanowires exclusively. Figure 2 depicts the SEM image and XRD diffraction pattern of the obtained material. Low-intensity diffraction peaks are observed at 2 values of 23.89°, 33.9°, 35.8°, 39.7° and 64.6°. They are indexed to (021), (002), (111), (130) and (152) copper hydroxide orthorhombic planes (JCPDS 13-420). The lattice constants were calculated as *a* = 2.88 Å, *b* = 11.03 Å and *c* = 5.03 Å, which are also in good agreement with the standard card. Based on these evidences, therefore, the nanowires structures correspond to Cu(OH)₂.

Figure 2 also displays the XRD patterns of the flower-like CuO grown on copper foil. The peaks located at 2 values of 35.6°, 38.7°, 67.2° and 67.9° correspond to the planes (002), (111), (311) and (113), respectively. Those belong to CuO

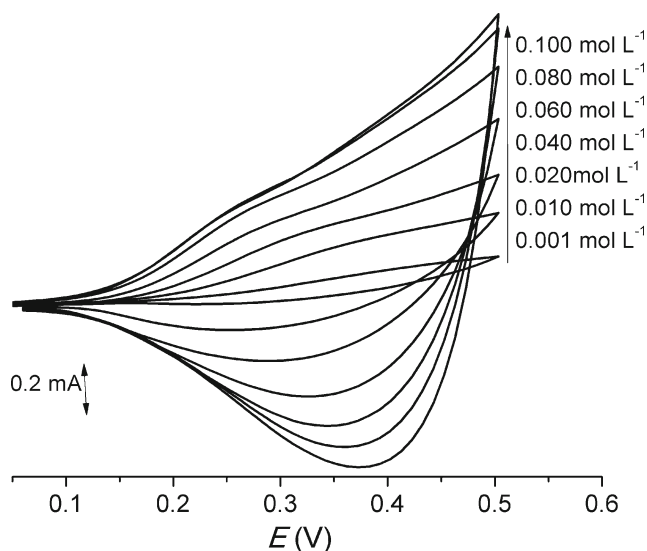


Fig. 5 CVs for the CuO electrode recorded at different concentrations of NaOH in the presence of 0.3×10^{-3} mol L⁻¹ and scan rate of 10 mV s⁻¹

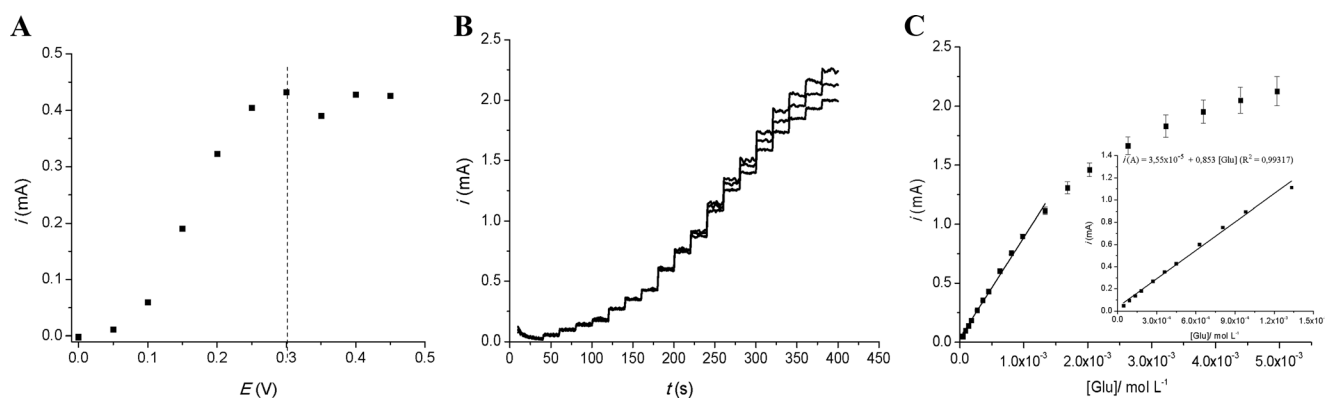


Fig. 6 **a** Current response as a function of applied potential in the presence of $1.0 \times 10^{-3} \text{ mol L}^{-1}$ glucose. **b** Amperometric curves obtained at a fixed potential of +0.30 V in the presence of different

concentrations of glucose. **c** Calibration curve of the CuO electrode, the inset shows the linear regression

monoclinic phase (JCPDS 45-937), with calculated lattice parameters is $c = 5.11 \text{ \AA}$. Furthermore, the grain size of 25 nm was calculated by using the Scherrer equation, $D_{hkl} = 0.89\lambda/\beta\cos\theta$, where λ is the wavelength of $\text{Cu}_{K\alpha}$ line ($\lambda = 0.15406 \text{ nm}$), θ is the Bragg diffraction angle of measured plane and β is the full width at half maximum (FWHM) of the (002) peak of CuO [21].

Figure 3 shows enlarged SEM images of the side view (a) and top view (b) where the hierarchical structure of the as-synthesized CuO can be seen clearly. At the bottom, assembly of thick branches constituted of stacked nanowires is developed. Over this structure, small and short branches highly interconnected arise leading to the formation of the 3D structure observed from the top view. As indicated by arrowheads, it seems that CuO also presents a preferential orientation growth.

Electrocatalytic activity of CuO electrode towards glucose oxidation

The electrocatalytic activity of the synthesized CuO nanostructures was evaluated by using cyclic voltammetry (CV). Figure 4a shows the CV curves of the electrode in 0.1 mol L^{-1} NaOH solution with the concentrations of glucose ranging

from 0 to $2 \times 10^{-3} \text{ mol L}^{-1}$ at a scan rate of 10 mV s^{-1} . The signals ascribed to the Cu(III)/Cu(II) redox couple that handles the glucose oxidation appear broad and poorly defined in the absence of glucose (dotted line). But as expected, a remarkable catalytic peak resulted by increasing the glucose concentration. The decrease in the cathodic current that occurs in the backward swept constitutes another evidence of the electrocatalytic activity of CuO towards glucose oxidation. Figure 4b exhibits the response of the untreated copper electrode in the absence and the presence of glucose as a comparison. There are differences in the voltammetric profiles; the oxidation potential of CuO electrode (dotted line) is less positive than the copper electrode as a consequence of the electrocatalytic effect while the current is similar. But it must take into consideration that this comparison is not entirely accurate because the measurement is carried out in an alkaline medium, which can promote the formation of the oxide on the surface of the copper electrode during the positive scan. The alkaline solution is necessary to ensure the electrocatalytic activity of CuO as shown in Fig. 5. The shape of the voltammetric curve greatly depends on the NaOH concentration; the peaks become more pronounced as the electrolyte concentration increased, which confirmed that the electrocatalytic oxidation of glucose involves the hydroxyl group ($-\text{OH}$). A maximum

Table 1 Comparison of the analytical performance of the as-prepared CuO electrode with other CuO non-enzymatic glucose sensors

Electrode	LOD ($\mu\text{mol L}^{-1}$)	Sensitivity $\mu\text{A } \mu\text{mol L}^{-1} \text{ cm}^{-2}$	Linear range ($\mu\text{mol L}^{-1}$)	Potential (V)	Reference
CuO nanocomposites/SWCNTs	0.05	1.61	0.05–1800	0.350 (vs. SCE)	[14]
Nafion/CuO nanoleaves/GCE	5.0	1.0	10–7300	0.700 (vs. SCE)	[22]
CuO/Cu nanowires/GCE	0.69	1.25	1–10,000	0.650 (vs. Ag/AgCl)	[23]
Cu foam	9.30	1.79	0.18–3470	0.500 (vs. Ag/AgCl)	[24]
CuO nanoparticles/carbon spheres/GCE	0.10	2.98	0.50–2300	0.550 (vs. SCE)	[25]
CuO nanoparticles/mesoporous carbons/GCE	0.10	1.15	0.4–7300	0.450 (vs. SCE)	[26]
CuO nanoparticles/carbon nanofibers/GCE	0.20	2.74	0.5–11,000	0.500 (vs. SCE)	[27]
Cuo nanoflowers/Cu foil	6.87	1.71	45.0–1330	0.300 (vs. SCE)	This work

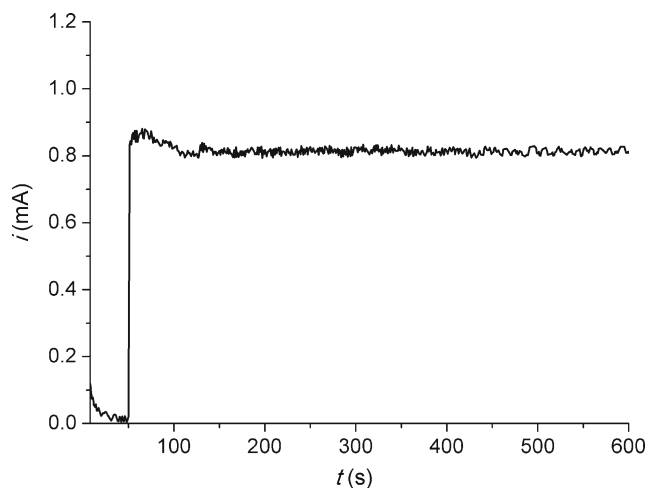
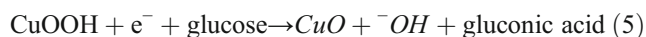


Fig. 7 Amperometric response of the CuO electrode in the presence of $5.0 \times 10^{-3} \text{ mol L}^{-1}$ glucose over 10 min at an applied potential of +0.30 V

peak current is reached at 0.1 mol L^{-1} NaOH, so this concentration was chosen for subsequent experiments. This fact can be explained considering the following reactions [9, 16]:



Amperometric determination of glucose

The amperometric response was preferred to assess the analytical performance of the CuO electrode. This technique is easy to use and furthermore shows low background current that is important to achieve higher sensitivity. Here, the applied potential is an important parameter that must be carefully selected to achieve a higher current at lower potential value; the latter is important to reduce the interferences from other

oxidizable species. Figure 6a shows the current responses registered as a function of the applied potential from 0 to 0.45 V in the presence of $1.0 \times 10^{-3} \text{ mol L}^{-1}$ glucose. A strong electrocatalytic activity becomes evident as the potential is shifted to more positive values, reaching a maximum current response at +0.3 V, so this potential was taken as the optimum potential. This value is quite similar to previously described CuO-based electrodes, but at least 100 to 200 mV less positive when compared with many others as shown in Table 1. The decrease in the overpotential suggests that the 3D hierarchical structure enhance the electron transfer reactivity of CuO.

Figure 6b shows the step-like amperometric responses of the CuO electrode with successive addition of glucose at an applied potential of +0.3 V; the average response of three repeated measurements was used to establish the calibration curve with 3 % RSD. As shown in Fig. 6c, the oxidation current is proportional to glucose concentration up to $1.33 \times 10^{-3} \text{ mol L}^{-1}$. The current response equation is $i \text{ (A)} = 3.55 \times 10^{-5} + 0.853 [\text{Glu}]$ with a correlation coefficient of 0.99317. The estimated limit of detection (LOD) is $6.9 \times 10^{-6} \text{ mol L}^{-1}$ based on $3\sigma/s$, where σ is the standard deviation of the blank currents ($n = 8$), and s is the slope of the calibration curve. The detection limit is lower than the normal blood glucose level ($6.1 \times 10^{-3} \text{ mol L}^{-1}$), indicating that the as-prepared CuO electrode is suitable for monitoring glucose in blood. The sensitivity of the CuO electrode is $1.71 \mu\text{A } \mu\text{mol}^{-1} \text{ cm}^{-2}$.

Stability, reproducibility and anti-interference of the CuO electrode

Three CuO electrodes prepared under the same conditions gave a 2.7 % RSD by measuring the peak current using cyclic voltammetry and 2.9 % taking the current registered by

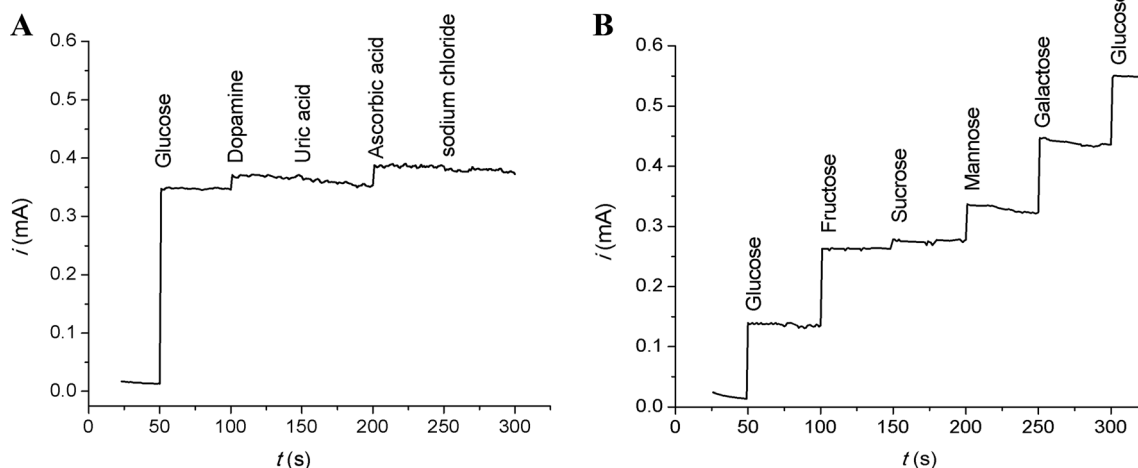


Fig. 8 a) Anti-interference test of the CuO electrode in 0.1 mol L^{-1} NaOH at an applied potential of +0.30 V in the presence of $1.0 \times 10^{-3} \text{ mol L}^{-1}$ followed by the addition of $1.0 \times 10^{-4} \text{ mol L}^{-1}$ DA,

UA, AA and NaCl. b) Amperometric response of $3 \times 10^{-4} \text{ mol L}^{-1}$ glucose in the absence and presence of $3 \times 10^{-4} \text{ mol L}^{-1}$ of fructose, sucrose, mannose and galactose

Table 2 Determination of glucose in serum samples and glucose recoveries

Sample	Reported in a local hospital (mmol L ⁻¹)	Proposed sensor (mmol L ⁻¹)	Glucose added (mmol L ⁻¹)	Found (mmol L ⁻¹)	Recovery (%)
1	5.33	5.72	0.101	0.102 ± 0.003	101
2	19.11	18.56	0.101	0.102 ± 0.006	101

chronoamperometry, indicating that the proposed method produced reliable and reproducible electrodes. Also, successive amperometric measurements yielded reproducible currents with the RSD of 3 %. Figure 7 shows the amperometric response of the CuO electrode in the presence of 5.0×10^{-3} mol L⁻¹ of glucose throughout an experiment prolonged for 10 min. The response remains constant during the experiment, a decrease of less than 2 % observed in the current indicates good stability. CuO is a highly stable electrode material and preserves its activity by storing in air at room temperatures.

The presence of some oxidizable biomolecules in blood that commonly co-exist with glucose may affect the electrode response. Thus, the anti-interference test was performed to evaluate the selectivity of the glucose sensor. Figure 8a shows the amperometric response of 1.0×10^{-3} mol L⁻¹ glucose, followed by the additions of 0.1×10^{-3} mol L⁻¹ of dopamine (DA), uric acid (UA) and ascorbic acid (AA). These concentrations were taken considering that the concentration of glucose in the healthy human blood is higher than these others. The small response of DA, UA and AA compared to glucose indicates that this electrode can selectively determine the glucose concentration in the coexistence of these interfering agents. The addition of 0.1×10^{-3} mol L⁻¹ of NaCl also does not cause interference. The CuO electrode exhibited similar electrocatalytic responses for other carbohydrates like fructose and galactose; this result is not surprising considering the mechanism involved in the oxidation. However, the electrode was less efficient for mannose and also showed only a slight catalytic current after the addition of sucrose; thereby exhibiting its ability for selective oxidation of sugars as shown in Fig. 8b.

Real Sample analysis

To evaluate the ability of the proposed sensor for routine analysis, 50 µL of serum samples were diluted with 25 mL of 0.1 mol L⁻¹ NaOH solutions. The amperometric response of glucose was recorded at a potential of +0.30 V and determined by the standard addition method. The results presented in Table 2 reveal good agreement with the glucose concentration determined by a routine enzymatic method in a regional hospital, with RSD of 7.3 and 2.9 %. Recovery studies also showed an insignificant matrix effect of the serum components in the glucose determination.

Conclusions

The oxidation of copper foil in NH₃-H₂O and NaOH solution is a simple, low-cost and reliable method that allowed the formation of flower-like CuO hierarchical nanostructures at room temperature. The as-prepared material was successfully applied as working electrode for electrochemical glucose detection. The high electrocatalytic activity, low limit of detection, high sensitivity and easy fabrication make this material a promising electrode in the development of a non-enzymatic glucose sensor. Also, the prepared electrode showed good stability and selectivity towards common interfering biological species.

Acknowledgments The authors acknowledge the financial supports from CNPQ (Process: 550441/2012-3), INCTBio (CNPq/INCT 573672/2008-3) and Propeq/UFRGS. The authors are also grateful to CAPES for the scholarship granted to the first author. The serum samples were donated by the Laboratory of Clinical Analysis of the Institute of Cardiology of Rio Grande do Sul, Porto Alegre-RS, Brazil.

References

- Sun YF, Liu SB, Meng FL, Liu JY, Jin Z, Kong LT, Liu JH (2012) *Sensors* 12:2610–2631
- Hahn YB, Ahmadwa R, Tripathy N (2012) *Chem Commun* 48:10369–10385
- Liu S, Sun S, You XZ (2014) *Nanoscale* 6:2037–2045
- Koffyberg FP, Benko FA (1982) *J Appl Phys* 53(2):1173–1177
- Ghijsen J, Tjeng LH, Van Elp J, Eskes H, Westerink J, Sawatzky GA (1988) *Phys Rev B* 38(16):11322–11330
- Yang Z, Wang D, Li F, Liu D, Wang P, Li X, Yue H, Peng S, He D (2013) *Mater Lett* 90:4–7
- Zhang Q, Zhang K, Xu D, Yang G, Huang H, Nie F, Liu C, Yang S (2014) *Prog Mater Sci* 60:208–337
- Zoolfakar AS, Rani RA, Morfa AJ, O'Mullane AP, Zadeh KK (2014) *J Mater Chem C* 2:5247–5270
- Huang F, Zhong Y, Chen J, Li S, Li Y, Wang F, Feng S (2013) *Anal Methods* 5:3050–3055
- Li X, Wei C, Fu J, Wang L, Chen S, Li P, Li H, Song Y (2014) *RSC Adv* 4:52067–52073
- Liu L, Chen Y, Lv H, Wang G, Hu X, Wang C (2015) *J Solid State Electr* 19:731–738
- Ibupoto ZH, Khun K, Beni V, Liu X, Willander M (2013) *Sensors* 13:7926–7938
- Kong C, Tang L, Zhang X, Sun S, Yang S, Song X, Yang Z (2012) *Anal Methods* 4:3174–3179
- Dung NQ, Patil D, Jung H, Kim D (2013) *Biosens Bioelectron* 42:280–286
- Jana S, Das S, Das NS, Chattopadhyay KK (2010) *Mater Res Bull* 45:693–698

16. Tian K, Prestgard M, Tiwari A (2014) *Mater Sci Eng C* 41:100–118
17. Toghiani KE, Compton RG (2010) *Int J Electrochem Sci* 5:1246–1301
18. Wen X, Zhang W, Yang S (2003) *Langmuir* 19:5898–5903
19. Liu J, Huang X, Li Y, Li Z, Chi Q, Li G (2008) *Solid State Sci* 10:1568–1576
20. Wang Y, Jiang T, Meng D, Kong J, Jia H, Yu M (2015) *RSC Adv* 5:16277–16283
21. Singh DP, Ojha AK, Srivastava ON (2009) *J Phys Chem C* 113:3409–3418
22. Zhao Y, Zhao J, Li Y, Ma D, Hou S, Li L, Hao X, Wang Z (2011) *Nanotechnology* 22:115604
23. Dong J, Ren L, Zhang Y, Cui X, Hu P, Xu J (2015) *Talanta* 132:719–726
24. Jiaojiao J, Yangyang G, Gangying Z, Yanping C, Wei L, Guohua H (2015) *Food Chem* 175:485–493
25. Zhang J, Ma J, Zhang S, Wang W, Chen Z (2015) *Sensors Actuators B Chem* 211:385–391
26. Zhang J, Zhu X, Dong H, Zhang X, Wang W, Chen Z (2013) *Electrochim Acta* 105:433–438
27. Zhang J, Ding N, Cao J, Wang W, Chen Z (2013) *Sensors Actuators B Chem* 178:125–131